The Establishment and Identification of a Humanized EV71 Virus Infection Model in Neonatal Mice

Guicai Liang[1,2], Lei Liu[2,*], and Chunlei Ge[1,*]

[1] Cancer Biotherapy Center, Yunnan Cancer Hospital, The Third Affiliated Hospital of Kunming Medical University, Peking University Cancer Hospital Yunnan, Kunming, China
[2] Jiamusi University, Jiamusi, Heilongjiang Province, China
Email: lguicai127@126.com (G.L.); liuleitianxue@163.com (L.L.); gechunlei1006@163.com (C.G.)
*Corresponding author

***Abstract*—Objective: To establish and validate a humanized EV71 (FY04-R5 C1-R4) virus infection model in neonatal BALB/c mice. Methods: The EV71 (FY04-R5 C1-R4) virus, propagated in RD cells (human rhabdomyosarcoma cells), was intraperitoneally injected into 1-day-old BALB/c neonatal mice. The mice were monitored for general condition, weight gain rate, histopathological changes, and the levels of VP1 mRNA and VP1 protein. The humanized EV71 virus infection model in neonatal mice was then characterized. Results: Compared with the control group, infected mice exhibited a significant decrease in body weight gain ($p < 0.05$). On day 3 post-infection, symptoms such as lethargy, reduced activity, and mental lethargy were observed. As the infection progressed, motor dysfunction in the hind limbs appeared, gradually worsening. By day 7, signs of ataxia, seizures, and hind limb paralysis were prominent. The levels of VP1 mRNA and VP1 protein in the brain and lung tissues of infected mice were significantly higher than those in the control group. Histological analysis revealed areas of necrosis and neuronal loss in the brain, and in the lung, thickening of the alveolar walls, enlarged and ruptured alveoli, and infiltration of inflammatory cells, including red blood cells. Conclusion: The intraperitoneal injection of EV71 (FY04-R5 C1-R4) virus successfully established a humanized EV71 infection model in neonatal BALB/c mice. This model provides an ideal platform for the study of Hand, Foot, and Mouth Disease (HFMD).**

***Keywords*—humanized EV71 virus, neonatal mice, model, validation**

I. Introduction

Hand, Foot, and Mouth Disease (HFMD) is a widespread viral infection, particularly prevalent in children, and is caused by more than 20 types of enteroviruses, with Enterovirus 71 (EV71) being the most significant [1]. EV71 is a non-enveloped RNA virus belonging to the Picornaviridae family, with viral particles measuring approximately 20-30 nm in diameter. The virus has a icosahedral symmetry and is composed of 60 identical subunits, each consisting of four structural proteins: VP1, VP2, VP3, and VP4, which encase the viral RNA genome [2–4]. Notably, VP1 is exposed on the virus surface and serves as a major target for the host immune response, containing key neutralizing epitopes that make it a useful biomarker for evaluating vaccine efficacy [5, 6].

Infection with EV71 typically presents acutely, with common symptoms including fever, oral pain, loss of appetite, and the appearance of vesicles or ulcers on the oral mucosa, along with rash on the hands, feet, buttocks, and legs [7, 8]. Severe cases may progress to complications such as encephalitis, meningitis, myelitis, circulatory failure, and pulmonary edema, which can be fatal or lead to significant long-term disability. The first major outbreak of EV71 occurred in Malaysia in 1997, resulting in 41 child deaths. From May 2008 to December 2011, mainland China reported over 5 million cases of HFMD, with 1,870 fatalities, and the incidence has continued to rise annually [9–11].

As humans are the primary host of EV71, the virus is transmitted primarily through direct contact with infected bodily fluids, including vesicular fluid and respiratory secretions. Under favorable environmental conditions, the virus can survive up to 72 hours, facilitating fecal-oral transmission. Clinically, EV71 infection is more likely to cause severe neurological complications and pulmonary edema compared to other enterovirus serotypes [12–14]. Neurogenic pulmonary edema, often a result of brainstem encephalitis, is particularly dangerous and can lead to rapid death in some cases. Survivors may experience significant sequelae. This form of pulmonary edema is not only due to systemic vasoconstriction and circulatory failure caused by brainstem injury but also results from increased vascular permeability in the lungs, leading to extensive erythrocyte extravasation due to systemic inflammatory responses [15].

Research on combating EV71 virus infection has garnered widespread attention both domestically and internationally. However, due to the incomplete understanding of the pathogenic mechanisms of EV71 and the lack of ideal animal models, progress in the development of effective prevention and treatment

Manuscript received November 2, 2024; revised December 5, 2024; accepted December 12, 2024; published December 30, 2024.

strategies has been slow [16]. In this study, we established an infection model through intraperitoneal injection. The model was evaluated based on general conditions, weight loss rate, histopathological changes, VP1 mRNA levels, and VP1 protein content. Our results confirm the successful establishment of the model, providing a solid foundation for the screening of EV71 vaccines, antibodies, and potential therapeutic drugs, as well as for studies on drug mechanisms of action.

II. Materials and Methods

A. Experimental Materials

1) Experimental animal

Sixty female and thirty male SPF-grade BALB/c mice, weighing between 18 and 22 grams, were purchased from Yisi Laboratory Animal Technology Co., Ltd., Changchun, China (license number: SCXK(Ji)-2016-0003). The mice were housed under controlled conditions: temperature ranged from 18 to 22°C, humidity from 40% to 80%, with a 12-hour light/dark cycle. They were kept in individual ventilated cage (IVC) systems at the Jiamusi University Laboratory Animal Facility. All feed, drinking water, and bedding materials were sterilized by autoclaving. The feed and water were replaced daily, while the bedding was changed twice weekly. The experimental procedures were conducted at the Jiamusi University Life Sciences Experimental Center, and all in vivo experiments were approved by the Jiamusi University Ethics Committee (Approval No. JMSU-224).

2) Virus collection

To establish RD cell cultures, the EV71 virus strain (FY04-R5 C1-R4) was inoculated onto a monolayer of RD cells. The cells were cultured in maintenance medium consisting of 2% serum (10% fetal bovine serum, 1% antibiotics, 1% glutamine) adjusted to a pH of 7.4, and incubated at 37°C with 5% CO_2. Once more than 80% of the cells showed evident cytopathic effects under microscopic observation, the cells were subjected to three freeze-thaw cycles. The culture supernatant was then collected and centrifuged at 3000 rpm for 5 minutes. The resulting supernatant was aliquoted and stored at −80°C.

3) Reagent

RNA extraction kits, reverse transcription kits, etc., were purchased from Baosheng Bioengineering (Dalian) Co., Ltd.; MEM culture medium was purchased from Nippon Surfactant Co., Ltd. (Japan); fetal bovine serum and antibiotics (penicillin-streptomycin) were purchased from GIBCO (USA); β-actin antibody, HRP-goat anti-rabbit IgG, HRP-goat anti-mouse IgG were purchased from Santa Cruz Biotechnology (USA); VP1 antibody was purchased from Abnova (Taiwan); ECL chemiluminescence reagent was purchased from Advansta (USA).

B. Method

1) Grouping and modeling of experimental animals

a) Experimental animal grouping

After adapting the purchased BALB/c mice to the breeding environment for one week, they were randomly divided into 30 cages, with 2 female mice and 1 male mouse per cage. They were then kept under normal conditions to mate freely. After two weeks of cohabitation, the mice were separated, and pregnant females were selected. From the 20 randomly chosen pregnant females, the pups born were designated as the control group (normal group), while the pups born from 30 other pregnant females were designated as the experimental group (virus group). All female mice were kept under normal conditions. The pups in the control group received intraperitoneal injections of physiological saline, while the pups in the virus group received intraperitoneal injections of humanized EV71 virus.

b) Establishment of an EV71 virus infection model in neonatal mice

Newborn mice from the virus group, aged 1 day, were separated from their mothers and fasted (both food and water) for 4 hours. A humanized EV71 viral suspension was retrieved from the −80°C freezer. The mice were positioned with their abdomen facing upward, head lowered and tail raised to fully expose the abdomen. A 1/3 section of the lateral abdominal wall was selected for needle insertion. The needle was carefully advanced about 5 mm under the skin along the abdominal wall, crossing the midline to the opposite side, and the viral suspension (50 μL) was injected into the peritoneal cavity. The needle was withdrawn slowly and gently rotated, and the injection site was pressed with a hemostatic cotton swab, followed by gentle massage for 3 minutes to promote absorption and prevent leakage. The general condition and body weight of the mice were monitored daily.

c) Collection of specimens

Tissues from the brain and lungs were collected at five time points: day 3, day 5, day 7, day 10, and day 14 post-injection for nucleic acid, protein, and pathological analyses.

2) Viral load measurement

a) Determination of viral VP1 mRNA

Total RNA was extracted from the brain and lung tissues of normal and experimental group neonatal mice at five time points post-virus inoculation. RT-PCR was performed for reverse transcription, amplification, agarose gel electrophoresis, and image analysis. The VP1 primer sequences were as follows: F: GATACAGGCAAGGTTCCAGCACTC; R: GCGTGTCTCAATCATGCTCTCGTC. The amplification conditions were as follows: 94°C for 30 s, 55°C for 30 s, 72°C for 30 s, followed by 25 cycles, with a final extension at 72°C for 2 min.

b) Determination of virus VP1 protein

Total protein was extracted from the brain and lung tissues of normal and experimental group neonatal mice at five time points post-virus inoculation. VP1 protein levels were measured by Western blot. Tissue total protein was extracted, separated by SDS-PAGE, and transferred to a membrane at 260 mA for 50 minutes. After blocking, primary antibodies (β-actin 1:1000, VP1 1:1000) were incubated overnight at 4°C. Secondary antibody (IgG 1:10,000) was incubated at 37°C for 1 hour, followed by

ECL detection. The protein density ratio of VP1 to the internal reference β-actin (A, OD) was subjected to statistical analysis.

3) Histopathological examination

Brain and lung tissues from neonatal mice were fixed in formaldehyde, dehydrated in ethanol, embedded in paraffin, sectioned, and deparaffinized with xylene, followed by H&E staining.

C. Statistical Method

Quantitative data are expressed as mean ± Standard Deviation (SD). One-way analysis of variance (ANOVA) was performed using GraphPad Prism 9 statistical software, with a significance level of $p < 0.05$ considered statistically significant.

III. Results

A. General Condition of Suckling Mice

Observation of the status of neonatal mice following viral infection: Neonatal mice in the control group showed no apparent adverse symptoms at any time point. In the virus group, mice began to exhibit symptoms such as reduced activity, sparse fur, and lethargy starting on day 3 post-EV71 virus inoculation. By day 5, symptoms such as weight loss, drowsiness, hind limb paralysis, and even seizures were observed (Fig. 1A). Weight changes of neonatal mice in the control and virus groups at five time points after infection (Fig. 1B). Mice in the control group continued to gain weight, with an increasing rate of growth, consistent with the normal growth pattern of animals. In the virus group, the weight gain rate on day 3 post-infection showed no significant difference compared to the control group ($p > 0.05$). However, from day 7 onwards, the weight gain rate began to decrease significantly, showing a notable difference compared to the control group ($p < 0.05$). After day 7 post-infection, neonatal mice in the virus group began to die, whereas no deaths were observed in the control group.

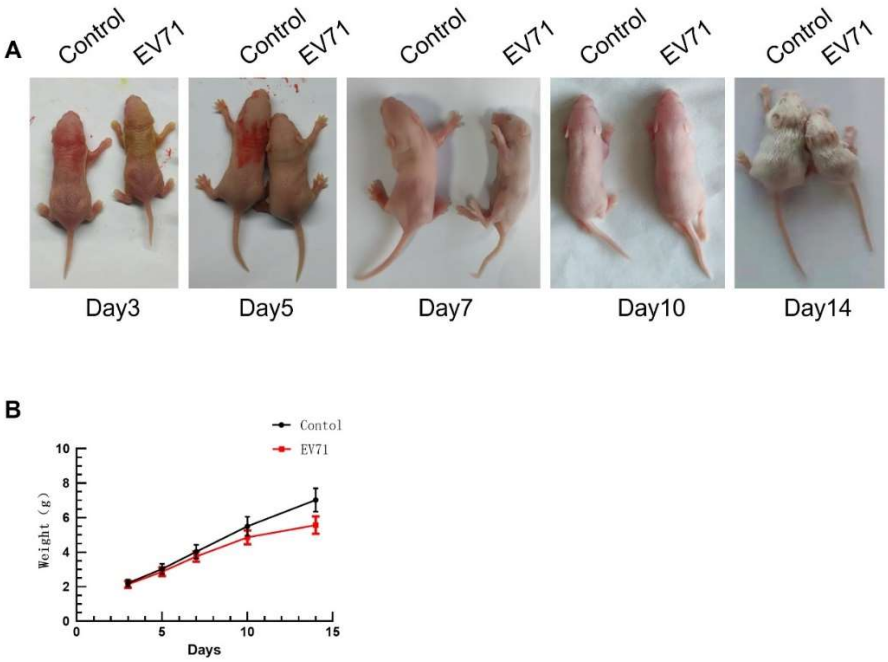

Fig. 1. A: Comparison of Normal Suckling Rats and Infected Suckling Rats at 5 Time Points after Infection with Virus. B: Weight changes of suckling mice in normal and experimental groups at five time points.

B. Determination of VP1 mRNA of EV71 Virus

No EV71 virus VP1 mRNA was detected in the brain and lung tissues of neonatal mice in the control group. The ratios of VP1 mRNA to housekeeping gene expression in the brain and lung tissues of neonatal mice in the virus group are as follows: Virus group brain: Day 3, 0.41 ± 0.039; Day 5, 0.50 ± 0.042; Day 7, 0.62 ± 0.061; Day 10, 0.54 ± 0.051; Day 14, 0.58 ± 0.055; Virus group lung: Day 3, 0.43 ± 0.041; Day 5, 0.52 ± 0.049; Day 7, 0.66 ± 0.060; Day 10, 0.60 ± 0.057; Day 14, 0.53 ± 0.051. Compared to the experimental group at day 3, there was no significant increase in VP1 mRNA levels on day 5 ($p > 0.05$). However, a significant increase was observed on days 7, 10, and 14 ($p < 0.05$) (Fig. 2).

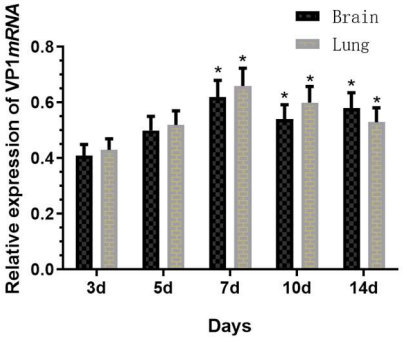

Fig. 2. Replication of EV71 mRNA in brain and lung tissues of suckling mice in virus group.

C. Determination of VP1 Protein of EV71 Virus

EV71 virus VP1 protein was not detected in the brain and lung tissues of neonatal mice in the control group. In the experimental group, VP1 protein expression was observed at all five time points post-inoculation in both brain and lung tissues, with VP1 protein levels in the lung tissue being higher than in the brain tissue, although this difference was not statistically significant ($p > 0.05$). Compared to the experimental group at day 3, there was no significant increase in VP1 protein levels on day 5 ($p > 0.05$), but significant increases were observed on days 7, 10, and 14 ($p < 0.05$) (Fig. 3).

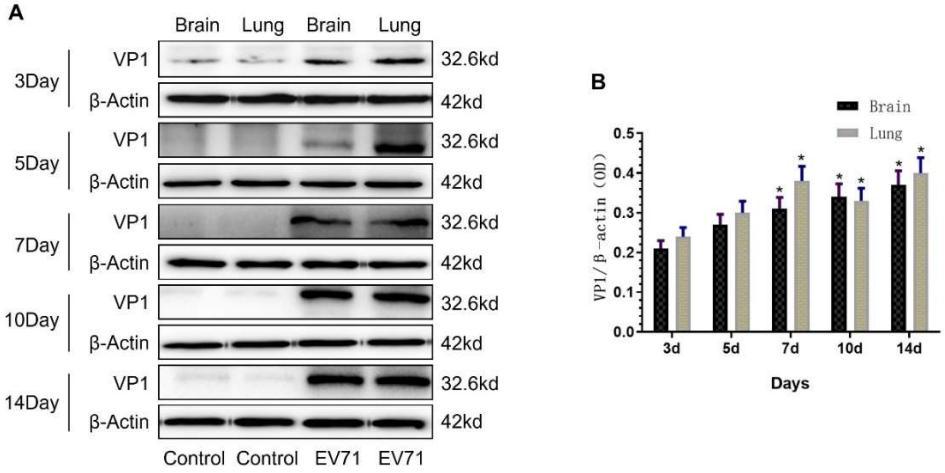

Fig. 3. Protein expression of VP1 in brain and lung tissues of suckling mice in virus group at different time points.

D. HE Staining of Lung and Brain Tissue

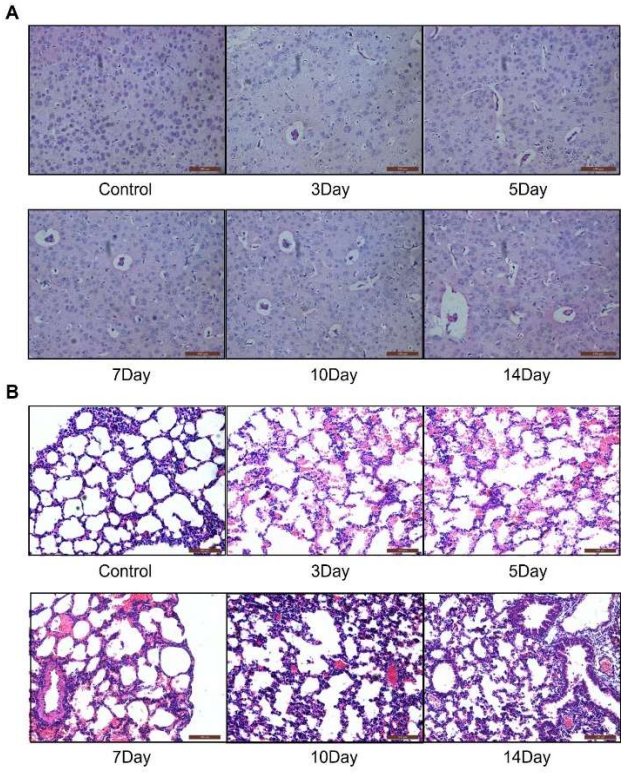

Fig. 4. A: Pathological sections of brain tissue of suckling mice infected with EV71 virus (× 200). B: Pathological section of lung tissue of suckling mice infected with EV71 virus (× 200).

Hematoxylin and Eosin (HE) staining was performed on the brain and lung tissues of neonatal mice at five different time points following EV71 virus inoculation. In the control group, no significant pathological changes were observed in brain and lung tissues across all five time points. In contrast, the virus-inoculated group exhibited notable pathological alterations: brain tissue showed liquefactive and softening necrosis, marked congestion of the brain parenchyma, a reduction in the number of neurons, and a considerable presence of necrotic neuronal cells along with neuronophagia. The lung tissue demonstrated pronounced pulmonary edema, enlargement and rupture of alveoli, significant thickening of the alveolar walls, and was accompanied by extensive inflammatory cell infiltration and erythrocyte extravasation, resulting in mild congestion (Fig. 4).

IV. Discussion

EV71 virus was first discovered in 1969, but it wasn't until after 1998 that research on this virus began to increase significantly, largely due to the major outbreaks of Hand, Foot, and Mouth Disease (HFMD) in the Asia-Pacific region between 1997 and 1998 [17]. Studies on EV71 virus typically use 7-day-old neonatal mice as animal models, as older mice develop resistance to the virus, which is consistent with the clinical observation that EV71 infections are most common in children under five years old [18, 19].

In this study, a humanized EV71 virus was administered via intraperitoneal injection, and the virus infection was assessed by VP1 mRNA and VP1 protein detection, along with histopathological examination. A successful EV71 infection model in neonatal mice was established through intraperitoneal injection, confirming that the humanized EV71 virus is pathogenic in humans and can also infect neonatal mice. Previous studies have established EV71 infection models in neonatal mice using intracranial or intrathecal injections, but these methods cause significant harm to the mice and result in higher mortality rates [20]. In contrast, intraperitoneal injection not only simplifies the

procedure but also causes less harm to the mice, making it a preferable method for establishing EV71 infection models in neonatal mice [21]. Additionally, the humanized EV71 virus theoretically reduces its mutation rate, providing a better experimental subject for the development of antibodies or vaccines for HFMD research [22].

Upon detection of VP1 mRNA and VP1 protein, a decrease in viral load was observed on day 10. However, the viral load increased again by day 14, possibly due to the host's immune response against the EV71 virus beginning seven days post-infection. However, the immune response mechanisms following EV71 infection remain unclear and warrant further investigation [23].

EV71 is a single-stranded positive-sense RNA virus. The mechanisms of its neurotoxic effects remain poorly understood. Studies suggest that the virus may directly invade neural tissue and/or induce a series of stress responses in the nervous system following infection. In this study, we observed clear pathological changes in brain tissue, including softening lesions, neuronal loss, necrosis, and neuronophagia, indicating that EV71 is neurotropic and can lead to neurocytolysis [24]. Furthermore, one study has observed that EV71 virus targets specific neuronal cells, leading to localized inflammation in specific regions of the nervous system. The virus may enter the nervous tissue via the bloodstream, crossing the blood-brain barrier and damaging certain areas of the brain [25]. Since the blood-brain barrier in infants is not fully developed, the virus is more likely to cross it, potentially leading to conditions such as meningitis and encephalitis in young children. Pulmonary edema is also a major complication in severe cases of EV71 infection. In our experimental group, neonatal mice exhibited significant pathological changes in lung tissue, including pulmonary edema, thickened alveolar walls, and inflammation [26]. Currently, the pathophysiology of pulmonary complications due to EV71 infection remains incomplete, and it is unclear whether the observed pathological changes are due to viral accumulation or the inflammatory response, requiring further investigation [27].

There are several limitations in this study. First, to prevent cross-contamination of the virus through respiratory routes, the control and virus-infected groups of neonatal mice were obtained from different mothers [27]. Second, while we observed paralysis of the hind limbs in virus-infected neonatal mice, we did not examine the hindlimb tissues, so it remains uncertain whether the paralysis is due to viral accumulation in muscle tissue or nerve damage. Further investigations are needed to clarify the cause [28].

In summary, this study successfully established an EV71 infection model in neonatal mice through intraperitoneal injection of humanized EV71 virus, demonstrating clear symptoms of infection and distinct pathological changes in the brain and lung tissues. This model lays the foundation for further research into the pathogenesis of EV71 and the development of therapeutic strategies.

Conflict of Interest

The authors declare that the research was conducted in the absence of any commercial or financial relationships that could be construed as potential conflicts of interest.

Author Contributions

All the authors contributed to the article. GL wrote the manuscript with support from LL and CG; LL performed the data analysis and data interpretation; CG supervision and revision of the manuscript; all authors had approved the final version.

Funding

This study was supported in part by grants from the National Natural Science Foundation of China (No. 82260462).

References

[1] S. Singh, V. T. K. Chow, M. C. Phoon, K. P. Chan, and C. L. Poh, "Direct detection of Enterovirus 71 (EV71) in clinical specimens from a hand, foot, and mouth disease outbreak in Singapore by reverse transcription-PCR with universal enterovirus and EV71-specific primers," *J. Clin. Microbiol*, vol. 40, no. 8, pp. 2823–2827, 2002.

[2] A. J. Aw. (2014). Activation and regulation of IL-1β family of cytokines by EV71 infection. [Online]. Available: https://dr.ntu.edu.sg/handle/10356/60262

[3] W. De, K. Changwen, L. Wei, *et al.*, "A large outbreak of hand, foot, and mouth disease caused by EV71 and CAV16 in Guangdong, China, 2009," *Archives of Virology*, vol. 156, no. 6, pp. 945–953, 2011.

[4] J. Xu, Y. Qian, S. Wang, *et al.*, "EV71: An emerging infectious disease vaccine target in the Far East?" *Vaccine*, vol. 28, no. 20, pp. 3516–3521, 2010.

[5] L. Longding, Z. Ying, W. Jingjing, *et al.*, "Study of the integrated immune response induced by an inactivated EV71 vaccine," *Plos One*, vol. 8, no. 1, e54451, 2013.

[6] L. Liu, H. Zhao, Y. Zhang, *et al.*, "Neonatal rhesus monkey is a potential animal model for studying pathogenesis of EV71 infection," *Virology*, vol. 412, no. 1, pp. 91–100, 2011.

[7] K. Fujii, N. Nagata, Y. Sato, *et al.*, "Transgenic mouse model for the study of enterovirus 71 neuropathogenesis," *Proc. Natl. Acad. Sci. USA*, vol. 110, no. 36, pp. 14753–14758, 2013.

[8] X. Menghua, S. Liyun, C. Lingfeng, *et al.*, "Genotypes of the enterovirus causing hand foot and mouth disease in Shanghai, China, 2012–2013," *Plos One*, vol. 10, no. 9, e0138514, 2015.

[9] G. Soren, Y. Lena, T. R. Kollmann, *et al.*, "Implications of age-dependent immune responses to enterovirus 71 infection for disease pathogenesis and vaccine design," *Journal of the Pediatric Infectious Diseases Society*, no. 2, pp. 162–170, 2013.

[10] S. Dang, N. Gao, Y. Li, *et al.*, "Dominant CD4-dependent RNA-dependent RNA polymerase-specific T-cell responses in children acutely infected with human enterovirus 71 and healthy adult controls," *Immunology: An Official Journal of the British Society for Immunology*, 2014.

[11] Y. Du, Y. Xia, Y. Zou, *et al.*, "Exploiting the lymph-node-amplifying effect for potent systemic and gastrointestinal immune responses via polymer/lipid nanoparticles," *ACS Nano*, 2019.

[12] Y. Xia, J. Wu, Y. Du, *et al.*, "Bridging systemic immunity with gastrointestinal immune responses via oil-in-polymer capsules," *Advanced Materials*, vol. 30, no. 31, 1801067, 2018.

[13] S. T. Luo, W. Y. Chung, L. N. T. Nhan, *et al.*, "Hospital-based surveillance of enterovirus 71 in HCM City, Vietnam, 2011–2014," *International Journal of Infectious Diseases*, vol. 45, no. 1, 303, 2016.

[14] Y. Hai-Ying, W. Feng-Bin, W. Jiang-Rong, *et al.*, "Epidemiological study and clinical analysis of 98 patients with hand, foot and mouth

disease," *Journal of Microbes and Infection*, vol. 4, no. 1, pp. 22–25, 2009.
[15] L. Jiang, R. Fan, S. Sun, *et al.*, "A new EV71 VP3 epitope in norovirus P particle vector displays neutralizing activity and protection in vivo in mice," *Vaccine*, vol. 33, no. 48, pp. 6596–6603, 2015.
[16] S. Dang, N. Gao, Y. Li, *et al.*, "Dominant CD4-dependent RNA-dependent RNA polymerase-specific T-cell responses in children acutely infected with human enterovirus 71 and healthy adult controls," *Immunology*, vol. 142, no. 1, 2014.
[17] C. S. Chen, Y. C. Yao, S. C. Lin, *et al.*, "Retrograde axonal transport: A major transmission route of enterovirus 71 in mice," *Journal of Virology*, vol. 90, no. 17, pp. 8996–9003, 2007.
[18] J. F. Han, R. Y. Cao, T. Jiang, *et al.*, "Echovirus 30 in EV71-associated hand, foot and mouth disease outbreak, Guangxi, China," *Journal of Clinical Virology the Official Publication of the Pan American Society for Clinical Virology*, vol. 50, no. 4, pp. 348–349, 2011.
[19] H. B. Hsiao, A. H. Chou, S. I. Lin, *et al.*, "Delivery of human EV71 receptors by adeno-associated virus increases EV71 infection-induced local inflammation in adult mice," *Biomed Research International*, vol. 2014, no. 3, 878139, 2015.
[20] Z. Liang and J. Wang, "EV71 vaccine, an invaluable gift for children," *Clinical & Translational Immunology*, 2014.
[21] J. Wang, J. Pu, H. Huang, *et al.*, "EV71-infected CD14(+) cells modulate the immune activity of T lymphocytes in rhesus monkeys," *Emerging Microbes & Infections*, 2013.
[22] L. Zhilan, W. Huan, and Z. Zhanglan, "EV71 virus infected with hand, foot and mouth disease combined MRI diagnostic progress of nervous system damage," *Journal of Imaging Research and Medical Applications*, 2017.
[23] L. I. Bingjie, "Study on the sensitivity of intestinal virus EV71 in different cells," *Journal of Shanxi Medical University*, 2015.
[24] W. C. Ch'ng, E. J. Stanbridge, K. Ong, *et al.*, "Partial protection against Enterovirus 71 (EV71) infection in a mouse model immunized with recombinant newcastle disease virus capsids displaying the EV71 VP1 fragment," *Journal of Medical Virology*, vol. 83, no. 10, 2011.
[25] N. Lazouskaya, E. Palombo, and P. Barton, "Poster: The cell culture status affects rescue of EV71 from in vitro RNA transcripts," presented at ASBMB's Special Symposium "Recent Advances in Pathogenic Human Viruses", Guangzhou, China, 2011.
[26] K. A. Stellrecht, D. M. Lamson, and J. R. Romero, "Enteroviruses and parechoviruses," *Manual of Clinical Microbiology*, pp. 1536–1550, 2015.
[27] C. T. Hung, Y. A. Kung, M. L. Li, *et al.*, "Additive promotion of viral internal ribosome entry site-mediated translation by far upstream element-binding protein 1 and an enterovirus 71-induced cleavage product," *PLoS Pathogens*, vol. 12, no. 10, e1005959, 2016.
[28] Q. Y. Mao, Y. Wang, L. Bian, *et al.*, "EV71 vaccine, a new tool to control outbreaks of Hand, Foot and Mouth Disease (HFMD)," *Expert Review of Vaccines*, p. 599, 2016.